Monte Carlo simulation of solute aggregation on domain boundaries in binary alloys: Domain-boundary segregation and domain growth

J.-M. Liu*
Institute of Materials Research and Engineering, Lower Kent Ridge Road, Singapore 119260;
Laboratory of Solid State Microstructures, Nanjing University, Nanjing 210093, People's Republic of China;
and Department of Physics, National University of Singapore, Singapore 119260
(Received 1 December 1997)

Solute aggregation phenomena such as domain-boundary segregation and precipitation in binary alloys are studied by Monte Carlo simulation in a two-dimensional square lattice. The thermodynamic approach starts from the kinetic spin-exchange Ising model and the Q-state Potts model. Each lattice site is imposed with two lattice spin parameters. The Ising lattice is used to realize the solute diffusion event via spin exchange and the Potts model is applied to simulate a domain growth event via spin adjustment. An approach of the coupling kinetics between the two events is developed. In this paper we simulate the kinetics of domain-boundary segregation and domain growth in binary solid solutions. Severe domain-boundary segregation in systems where the solutes prefer energetically to stick on the boundaries is demonstrated. The kinetics of segregation depends on the Ising interaction parameters, and is characterized with the spatial correlation of the solutes. The solute segregation severely pins the domain boundaries. When the domain boundaries exhibit high migration ability, the domain-boundary segregation becomes less serious. Finally, we demonstrate the scaling property of domain growth in the present system, whereas growth of the average domain area shows negative deviation from the normal linear kinetics. [S0163-1829(98)01826-8]

I. INTRODUCTION

Many technologically important properties of polycrystalline materials are very sensitive to the distribution of solute atoms or clusters as well as defects like domain boundaries. The solute distribution shows quite different kinetic behaviors, depending more or less on the system parameters, such as temperature, composition, internal stress and external field as well. For example, we may achieve either a solid solution or a phase separated microstructure. A study of these phenomena constitutes one of the main fields of alloying thermodynamics and kinetics, and therefore has been attracting continued interest in last decade.[1]

The solutes distribute uniformly in a binary solid solution. For any point r in the crystal, in a time interval $t \gg \tau$, the characteristic diffusion time, one finds a solute atom with a probability

$$P(r) = C_0, \tag{1}$$

with C_0 being the alloy composition. One may relate the correlation length of the solutes to term $\lambda_0 \propto C_0^{-1}$. This is the only length to be taken into account in evaluating the property of binary solid solutions.

When we deal with a polycrystalline solid solution that consists of highly degenerated domains, the picture appears to be more complicated. First, it is the second length that must be taken into account, i.e., the average domain size (here we choose the average domain area $\langle A \rangle$). Due to the excess free energy associated with the domain boundaries (DBs), these degenerated domains will evolve through growth of the larger domains in concert with shrinking of the smaller ones.[2–5] It is now established that the domain size exhibits a single-peaked distribution and follows the scaling concept.[5–8] Such a distribution, $f(A,t)$, is defined by the probability that one may find at any point a domain of area A with respect to $\langle A \rangle$. Therefore, the scaling function $F(A/\langle A \rangle)$ can be formulated as[4]

$$F(A/\langle A \rangle) = f(A/\langle A \rangle, t), \tag{2}$$

with $\langle A \rangle$ obeying[4–9]

$$\langle A \rangle \propto t. \tag{3}$$

Therefore, in a polycrystalline solid solution there appear two characteristic scales of the microstructure, λ_0 and $\langle A \rangle$. Furthermore, solute segregation on the DBs of materials is a common phenomenon for materials processing.[10–14] Because of this, $P(r) < C_0$ as r points inside one domain. It is well known that the segregated solutes pin the DBs from movement.[14] This coupling leads to a significant difference in both λ_0 and $\langle A \rangle$ from the original values. Therefore, it is of special interest to have a deep understanding of domain-boundary segregation and related phenomena, such as domain growth kinetics in coupling with the segregation.

In fact, the problem of domain-boundary segregation cannot be more emphasized in engineering materials applications. Although the experiments related to these phenomena have frequently been the subject of intensive research,[10–14] up to now the applicable theoretical approach of this problem may still not be satisfactory since it consulates many assumptions. A number of microscopic techniques have been developed to probe the domain-boundary segregation, but the quantitative data are still not sufficient. Therefore, computer simulations of the solute aggregation in polycrystalline materials appears to be a powerful tool for reaching a deep

understanding of the problem, if only a pure diffusion sequence is considered without considering lattice reconstruction.

In this paper we will propose a thermodynamic model and develop a new Monte Carlo (MC) algorithm for studying the domain-boundary segregation in binary solid solutions. We leave a simulation of the domain-boundary precipitation to be described elsewhere. It is the standard way to model diffusion in a solid solution via the kinetic spin-exchange Ising model[15] where the diffusion event is simulated by constructing a Markov sequence and utilizing the well-known Metropolis algorithm of importance sampling.[16] Although vacancies play a crucial role for a diffusion event, it was verified that this role does not change the qualitative conclusion achieved in the direct spin-exchange model. The conventional statistical approach of the domain growth is the Q-state Potts model[17] that imposes each lattice site with one of the Q states ($Q \geqslant 2$). We will start from the two models and propose a MC approach of the domain-boundary segregation in concert with domain growth. Many interesting properties of the domain-boundary segregation and the domain growth will be revealed in our approach.

In Sec. II of this paper we will propose a thermodynamic model of our system and develop a MC algorithm. The simulated results are presented in Sec. III with extended analysis. The conclusion is given in Sec. IV.

II. MODEL AND SIMULATION PROCEDURE

A. Model

The simulation starts from a two-dimensional squared $L \times L$ lattice with the periodic boundary conditions applied. It is expected that the conclusion may be extended to the three-dimensional case. According to the Ising model, each site of the lattice is occupied by either species A or B, with the spin state $S_i = 0$ for A and $S_i = 1$ for B. The species B is treated as solute in the lattice. The alloy composition is then expressed as $C_0 = N_B/(N_A + N_B)$, where N_A and N_B ($N_A + N_B = N$) are the numbers of species A and B in the lattice, respectively. The neighboring spins are permitted to exchange in order to simulate lattice diffusion. In the present system, only the nearest-neighboring interaction is considered. The Ising Hamiltonian of the system has the well-defined form[18]

$$H_I = -\sum_{\langle ij\rangle} E_I = -\left[\phi_{AA}\sum_{\langle ij\rangle}(1-S_i)(1-S_j) + \phi_{BB}\sum_{\langle ij\rangle} S_iS_j + \phi_{AB}\sum_{\langle ij\rangle} S_i(1-S_j) + (1-S_i)S_j\right], \tag{4}$$

where E_{I} represents the Ising interaction of site i with its four nearest neighbors, ϕ_{mn} ($m,n = A,B$) denotes the interaction of the nearest-neighboring spin pair; $\langle ij\rangle$ represents that over nearest neighbors is summed once. We may define an effective Ising interaction term $\phi = \phi_{AB} - (\phi_{AA} + \phi_{BB})/2$, which serves as a variable defining the homogeneous system stability against fluctuations.[19] Roughly speaking, the lattice keeps homogeneous configuration if $\phi \geqslant 0$, otherwise it will separate into two types of domains with one being A rich and the other B rich. The static and dynamic properties of Eq. (1) have been studied by computer simulations and analytical approaches.[18]

We need another type of spin configuration to define the orientation of a site when we deal with a lattice of highly degenerated states. Because of the existence of the DBs, the interaction between domains must be considered. The highly degenerated lattice is conventionally described by the standard Potts model of spin state number $Q \geqslant 3$.[17] Each site is then imposed on one of the Q Potts spins, i.e., $q = 0,1,2,...,Q-1$. A local closed area in which all sites have the same Potts spin constitute one domain. If we denote by J ($\geqslant 0$) the interaction factor associated with any Potts spin pair, the interaction between nearest-neighboring sites with $q = \alpha$ and β, respectively, can be formulated as

$$J_{\alpha\beta} = J\delta_{\mathrm{Kr}}, \tag{5}$$

where

$$\delta_{\mathrm{Kr}} = [1 + (Q-1)\overline{e^{\alpha}}\overline{e^{\beta}}]/Q$$

is the Kronecker δ function and $\overline{e^{\alpha}}$ ($\alpha = 0,1,...,Q-1$) are Q unit vectors pointing in the Q symmetric directions of a hypertetrahedron in $Q-1$ dimensions.[17] The problem here is complicated since different Potts interactions between the like-Ising spin pair and unlike-Ising spin pair should be considered. Now we denote by J_{mn} ($\geqslant 0$, $m,n = A,B$) as the Potts interaction between a site pair whose Ising spins are m and n, respectively. Furthermore, the like- and unlike-Ising spin pairs may have different interactions that depend on the difference of their Potts spin states, so one may define a fraction factor f_{mn} ($0 \leqslant f_{mn} \leqslant 1$) and rewrite Eq. (5) into

$$J_{\alpha\beta} = J[(1-f_{mn}) + f_{mn}\delta_{\mathrm{Kr}}]. \tag{6}$$

It is clear that if $f_{mn} = 0$, the Potts interaction between two neighboring sites of Ising spins m and n is independent of their Potts spin state. This is the ground state, which means that no matter what the Potts spin state, the energy stays the same. Therefore, the Potts Hamiltonian of the system can be written as

$$\begin{aligned} H_P = -\sum_{\langle ij\rangle} E_P = &-\sum_{\langle ij\rangle} J_{AA}(1-S_i)(1-S_j) \times [(1-f_{AA}) + f_{AA}\delta_{\mathrm{Kr}}(\alpha,\beta)] \\ &-\sum_{\langle ij\rangle} J_{BB}S_iS_j[(1-f_{BB}) + f_{BB}\delta_{\mathrm{Kr}}(\alpha,\beta)] \\ &-\sum_{\langle ij\rangle} J_{AB}[S_i(1-S_j) + (1-S_i)S_j] \times [(1-f_{AB}) + f_{AB}\delta_{\mathrm{Kr}}(\alpha,\beta)], \end{aligned} \tag{7}$$

where E_P stands for the Potts interaction of a site with its four nearest neighbors. The final Hamiltonian of the system is then

$$H=H_I+H_P=-\sum_{\langle ij\rangle}(E_I+E_P)$$
$$=-\Big[\phi_{AA}\sum_{\langle ij\rangle}(1-S_i)(1-S_j)+\phi_{BB}\sum_{\langle ij\rangle}S_iS_j+\phi_{AB}\sum_{\langle ij\rangle}S_i(1-S_j)+(1-S_i)S_j\Big]$$
$$-J_{AA}\sum_{\langle ij\rangle}(1-S_i)(1-S_j)[(1-f_{AA})+f_{AA}\delta_{\mathrm{Kr}}(\alpha,\beta)]$$
$$-J_{BB}\sum_{\langle ij\rangle}S_iS_j[(1-f_{BB})+f_{BB}\delta_{\mathrm{Kr}}(\alpha,\beta)]$$
$$-J_{AB}\sum_{\langle ij\rangle}[S_i(1-S_j)+(1-S_i)S_j]\times[(1-f_{AB})+f_{AB}\delta_{\mathrm{Kr}}(\alpha,\beta)]. \quad (8)$$

From Eq. (8) it is quite clear that the solute aggregation on the DBs is preferred as the B-B spin pair has a smaller f_{BB} than either f_{AA} or f_{AB} even if all J_{mn} are identical.

B. Monte Carlo algorithm

Equation (8) represents a statistical description of a lattice coupled with the Ising spins and the Potts spins. A study of the static property is complicated and tedious. A simulation of the dynamic property becomes easier. We will start from the importance sampling of the Metropolis algorithm[16] and focus on the dynamic property.

The dynamic sequence in the lattice includes both the Ising spin exchange and the Potts spin adjustment. Both events may occur simultaneously but the MC simulation treats one event once. For a randomly chosen site i, the Ising spin exchange is approved via the following probability:

$$P_I=\frac{\exp(-E_I/k_BT)}{\exp(-E_I/k_BT)+\exp(-E_P/k_BT)}, \quad (9)$$

where k_B is the Boltzmann constant and T is temperature. This is a partition between the Ising and Potts events of the sequence. Once an Ising event is chosen, it is then to determine which nearest neighbor will exchange the spin with it at site i. The conventional algorithm of the Metropolis importance sampling is to approve an exchange event between site i and one of its nearest neighbors that is chosen at random via the following probability:

$$P^I_{\mathrm{ex}}=\begin{cases}\exp(-\Delta E_I/k_BT) & \text{if } \Delta E_I>0,\\ 1 & \text{if } \Delta E_I\leqslant 0,\end{cases} \quad (10)$$

with ΔE_I the difference in the Ising and Potts interactions after and before the exchange. It should be noted that the change of the Potts interaction must be considered as well as the Ising exchange between two neighboring sites that belong, respectively, to two domains. We always suppose that such an Ising event is accompanied by a self-consistent adjustment of the Potts spins of the two sites. This means that an Ising spin exchange does not affect the domain-boundary location in the lattice. Here, we employ an improved importance sampling that was developed by Xiao and co-workers in their approach to crystal-growth modeling.[20,21] This sampling considers the correlation among all possible spin-exchange steps. There are five probabilities for the spin exchange $i\Leftrightarrow i'$ between site $i=\langle x,y\rangle$ and any of its four neighbors, i'. Therefore, i' can be $\langle x,y\rangle$, $\langle x-1,y\rangle$, $\langle x+1,y\rangle$, $\langle x,y-1\rangle$, or $\langle x,y+1\rangle$, respectively. Here, x and y are the lattice coordinates along x and y axes, respectively. The spin exchange $i\Leftrightarrow i'$ is approved by the following probability, which is normalized with the sum of all five probabilities:

$$P^I_{\langle i\Leftrightarrow i'\rangle}=\frac{\exp(-\Delta E_I/k_BT)}{\Sigma_{\langle i\Leftrightarrow i'\rangle}\exp(-\Delta E_I/k_BT)}. \quad (11)$$

It is clear that the most probable event is that of the smallest (may be negative) ΔE_I. This importance sampling should be more effective than Eq. (10).

Similarly, if a Potts event is chosen via the partition Eq. (9), we consider all of the five probabilities with which the Potts spin at site i switches to be the same as one of its four neighbors, including itself. Note here that the event is not the Potts spin exchange but spin replacement, so the total Potts spin states change with time. The spin parameter defined in the Potts lattice appears to be nonconserved. We write the probability via which the Potts spin at site i is taken over by itself or one of its four neighbors i':

$$P^P_{\langle i\Rightarrow i'\rangle}=\frac{\exp(-\Delta E_P/k_BT)}{\Sigma_{\langle i\Rightarrow i'\rangle}\exp(-\Delta E_P/k_BT)}, \quad (12)$$

where ΔE_P is the difference in the Potts and Ising interaction after and before the Potts spin adjustment.

C. Procedure of simulation

We propose following procedure of simulation. For the given lattice and system parameters, site i is chosen at random and its E_I and E_P and then P_I are calculated consequently. A random number R is generated and compared with P_I. If $R<P_I$, site i is approved to do the Ising spin exchange. Then $P^I_{\langle i\Leftrightarrow i'\rangle}$ is calculated via Eq. (11) and another random number R' is created to decide with which neighbor i' site i will exchange the spin state. If $R\geqslant P_I$, we come to the Potts event and $P^P_{\langle i\Rightarrow i'\rangle}$ is calculated by Eq. (12). We create once more a random number R'' and compare it with $P^P_{\langle i\Rightarrow i'\rangle}$ to decide which neighbor of site i will be chosen to take its Potts spin over that of site i. We complete a circle and then another event starts. This procedure is repeated until a given number of circles is reached. The time of simulation is scaled by a unit of mcs. One mcs represents a completed $L\times L$ circle. Typically, the simulation is carried out up to 3600 mcs and occasionally limited to be 1500 mcs. For each system, four runs of simulation starting from different seeds of random number generation have been made and the average values of the simulated data are presented below.

For comparison, we will study the morphology and kinetics of solute segregation in two cases. One (we say Case I) is dominated with the Ising events where the domain-boundary migration is kinetically slow (slow domain growth). The other case (Case II) is an assumed comparable probability for

TABLE I. The system parameters of interaction for Cases I and II.

	ϕ_{AA}/k_BT	ϕ_{BB}/k_BT	ϕ/k_BT	J_{mn}/k_BT	f_{AA}	f_{BB}	f_{AB}
Case I	0.00	0.00	0.02–1.40	1.20	1.00	0.00	0.90
Case II	1.20	1.20	0.02–1.40	1.20	1.00	0.00	0.90

both the Ising and the Potts events. This means that the domain boundaries have high migration ability. By our simulations some interesting specifications for the two cases will be revealed. We choose $C_0=0.10$, $Q=24$, $L=128$ and 256, with the other system parameters listed in Table I. The initial domain size ranges from 10 to 50 lattice units in dimension, with shape and size of the individuals defined at random.

Table I takes $f_{BB}=0$ for both cases I and II, predicting that the B-B pair occupies the ground state of the Potts interaction. The total energy will get down if the B-B pair sticks onto the DBs. In case I we have $E_I \ll E_P$, so the Ising event is greatly preferred. E_I appears to be comparable to E_P in case II, resulting in a comparable probability for the Ising and Potts events. In addition, as different values of ϕ/k_BT for each of cases I and II are chosen, the partition, Eq. (9), may vary a little since it is of a low C_0. This variation may not change so much the time scale of the simulation.

III. SIMULATED RESULTS AND ANALYSIS

A. Case I: slow domain-boundary migration

We first study case I. Figure 1 presents the snapshot pictures of the boundary configuration at several times for $\phi/k_BT=0.02$. Here the DBs are labeled with solid circle dots and the open circles represent solute B, leaving solvent A unlabeled. The solutes are exaggerated for clarity and the DBs are plotted for easy eye view. In most cases, only part of the lattice is displayed so that the DBs do not look nice. Please note that as $\phi/k_BT>0$, the lattice should be a homogeneous solid solution, as shown at $t=0$ in Fig. 1, where only occasionally are found some solutes on the DBs.

It is clearly shown in Fig. 1 that just after the beginning of the simulation the uniformly distributed solutes tend to segregate onto the DBs ($t=50$ mcs). This tendency appears to be very rapid in the initial period (<200 mcs) and then becomes roughly saturated, depending weakly on the system parameters. Viewing the pictures from $t=300$ mcs to 2700 mcs, one gets a much higher density of the solute occupation on the DBs than inside the domains. Serious solute segregation on the DBs is then demonstrated. Furthermore, one finds that the solute segregation appears to be nonuniform. Some domain boundaries have most of the sites occupied with the solutes, whereas the others are much less occupied or even free of the solutes. This nonuniformity reflects the effect of the high degenerated Potts spin states. One boundary exhibits high excess energy as the two adjunctive domains show a big difference in the spin state q, whereas some others behave like a small angle boundary.[6–9] The solutes prefer to segregate onto the DBs of high excess energy.

Looking at the time evolution of the domain-boundary segregation, one confirms the enhancing effect of the DBs as a rapid channel of the solute diffusion. As indicated by the arrows in Fig. 1, at $t=50$, 300, and 800 mcs, the boundary is helpful for the solute diffusion and the neighboring boundaries benefit from it and become seriously solute segregated. Those boundaries serving as channels normally have relatively low excess energy, although not the lowest.

On the other hand, domain growth through the boundary migration, as a parallel event of solute aggregation, is clearly identified, although the growth is quite slow. The domains are compact and roughly equiaxed due to the high value of Q. The large domains grow in concert with the shrinking of the small ones. Four-domain junctions created through the shrinking of smaller domains become unstable and each finally splits into two trijunctions. These are normal domain growth features.[3–5] The interesting point here is the pinning effect of the solutes on the domain-boundary migration. It is easily observed that those seriously solute-segregated DBs hold high stability against migration and do not change their position too much over a long period. When the smallest

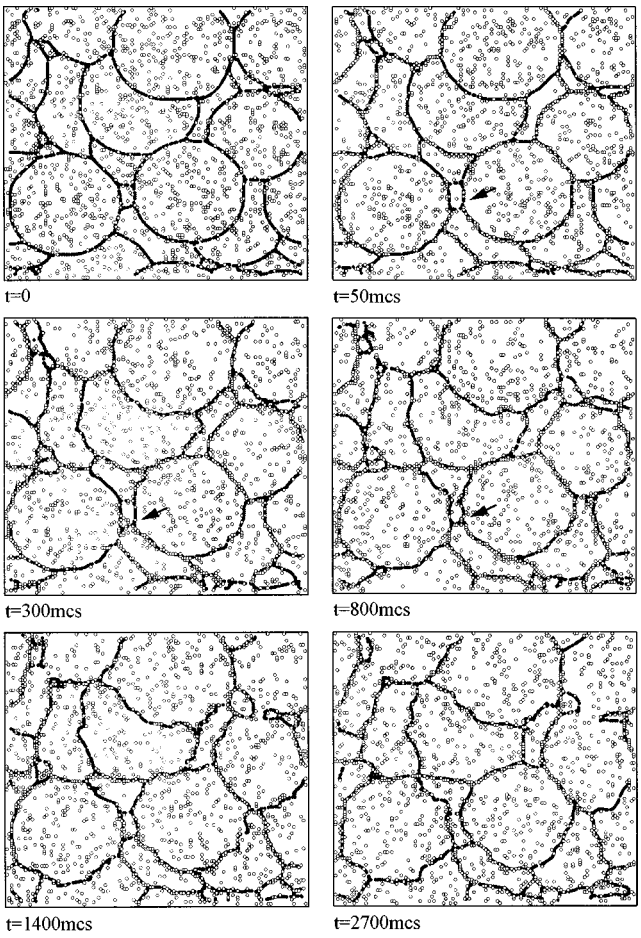

FIG. 1. The snapshot pictures of the domain-boundary configuration at several times indicated for case I. $L=128$ for the displayed range, $\phi/k_BT=0.02$. The solid spots are for the domain boundaries, the open spots are for the solute B and the empty area for the solvent A.

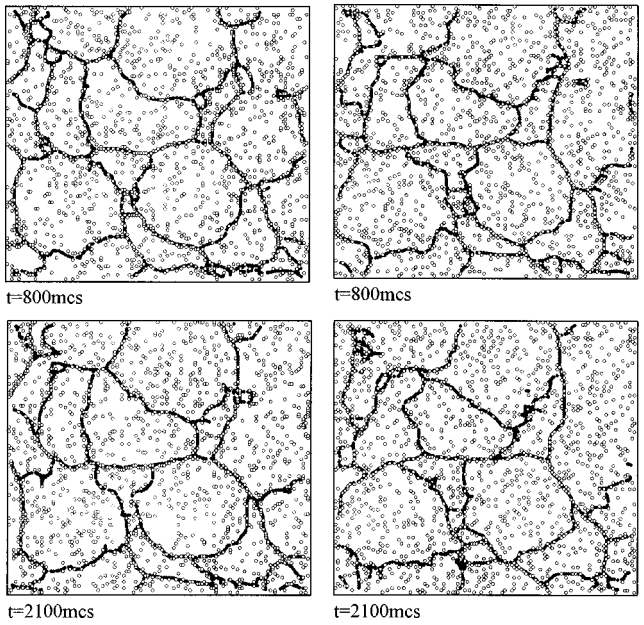

FIG. 2. The snapshot pictures of the domain-boundary configuration at several times indicated for case I. $L=128$ for the displayed range, $\phi/k_BT=0.20$ (left column) and 0.80 (right column).

domains finally disappear with time, a few of the domains that are small, but seriously B segregated on the DBs, still remain alive. The domain growth is mainly attributed to the migration of those DBs that are less solute occupied. The additional characteristic for the solute-pinned DBs is that they are not straight and smooth but are a little rippled, because they fluctuate in order to break the solute pinning and thus move.

The two columns in Fig. 2 show the snapshot pictures at $\phi/k_BT=0.20$ (left) and 0.80 (right). In reference to Fig. 1, similar behaviors are revealed, with some additional specifications. The first is that the domain-boundary segregation becomes less serious at a higher value of ϕ/k_BT. Looking at the right column, one finds that the occupation of the DBs by the solute is even higher at an early stage (after the initial sharp growth) than at the late stage. The second is reflected by the fact that the more serious irregularity of the domain boundary at a higher ϕ/k_BT is observed, compared to the case in Fig. 1. Since the pinning effect of the solutes still plays a role, the migration of the less solute-occupied DBs naturally lead to the rippled shape. This can be further confirmed in case II, to be presented below. The last point is the faster domain growth at the higher value of ϕ/k_BT, which can be clearly identified in Fig. 2.

We propose here a segregation coefficient of the DBs, Φ_{GB}, which is defined as

$$\Phi_{GB}=(C_{GB}-C_0)/C_{GB}, \tag{13}$$

where C_{GB} is the average composition over all boundary sites. If there is no boundary segregation, we have $\Phi_{GB}=0$, and $\Phi_{GB}=1-C_0$ if all boundary sites are occupied by the solutes. Figure 3 shows Φ_{GB} as a function of time for three values of ϕ/k_BT. As expected, Φ_{GB} increases quite sharply in the early stage and then tends to be saturated or even decays a little at a higher value of ϕ/k_BT. Note here that at

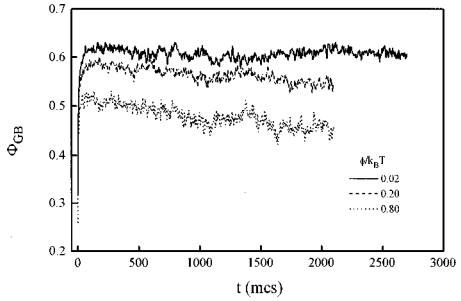

FIG. 3. The segregation coefficient Φ_{GB} as a function of time at several values of ϕ/k_BT for case I.

$\phi/k_BT=0.02$, Φ_{GB} reaches up to 0.62, not far from the maximum value, 0.90. In addition, the average energy per site, $\langle E\rangle$, also increases with time rapidly in the early stage and then slowly in the later stage. The higher ϕ/k_BT is, the lower $\langle E\rangle$ is, therefore the less serious the domain-boundary segregation is, as expected.

We evaluate the radially averaged correlation function of the solutes, $g(r,t)$, with r, the radial distance. The data at $t=800$ and 2700 mcs for $\phi/k_BT=0.02$ are plotted in Fig. 4(a). Although $g(r,t)$ shows considerable fluctuations against r, with an average fluctuation wavelength corresponding to λ_0, one observes an additional modulation of $g(r,t)$ against r. The modulation has its wavelength λ_1 not very much smaller than the average domain diameter. This fact indicates that the modulation is due to the domain-boundary segregation. That the wavelength at $t=2700$ mcs is larger than that at $t=800$ mcs results from the domain growth. The spatial correlation of the solutes $\lambda_0(t)$ for dif-

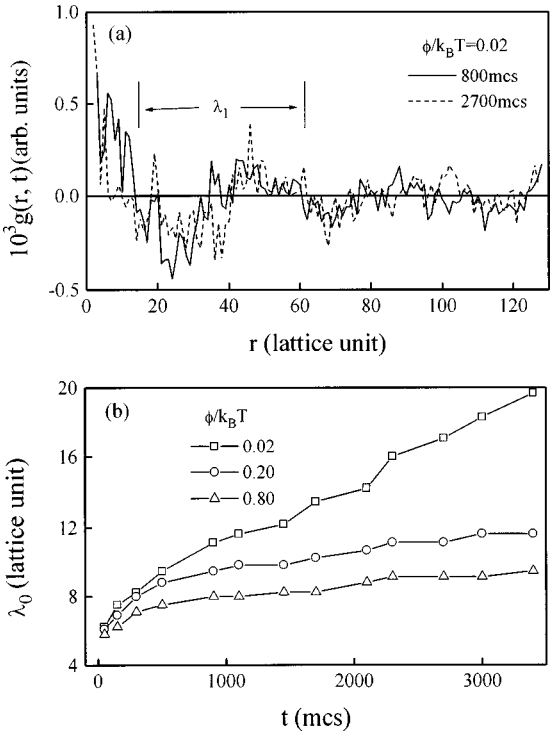

FIG. 4. (a) The radially averaged correlation function $g(r,t)$ as a function of distance r at $\phi/k_BT=0.02$ and (b) the fundamental wavelength λ_0 as a function of time at several values of ϕ/k_BT, for case I.

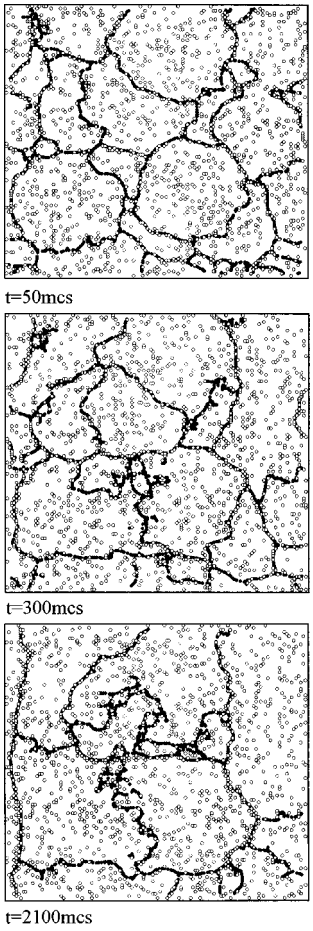

FIG. 5. The snapshot pictures of the domain-boundary configuration at several times indicated for case II. The displayed range $L=128$, $\phi/k_BT=0.20$.

ferent values of ϕ/k_BT are plotted against time in Fig. 4(b). In all cases, $\lambda_0(t)$ grows gradually. This growth is still detectable at a high value of ϕ/k_BT and is inferred to be attributed to the solute segregation on the DBs so that the solutes remaining inside the domains become diluted with time. As ϕ/k_BT becomes higher, the growth of $\lambda_0(t)$ may be negligible except from the very early stage.

B. Case II: comparable diffusion and boundary migration

Now we consider the case where the domain growth is comparable in kinetics to the solute diffusion, i.e., case II. At $\phi/k_BT=0.20$, the simulated results are presented in Figs. 5 and 6. From the snapshot pictures shown in Fig. 5, one still can identify significant segregation of the solutes onto the DBs once the process initiates. The more rapid the domain growth is, the weaker the boundary segregation is. At a similar time scale, the domain size at case II is much larger than that at case I. Toward the late stage ($t=2100$ mcs), only a few big domains remain in the lattice, with the other domains being swallowed by the larger ones. The weak segregation is attributed to the rapid migration of the DBs so that they do not have enough time to trap so many solutes. Another point that needs to be mentioned is that those less solutes-segregated DBs become seriously rippled in shape whereas the segregated DBs keep roughly straight. It is argued that the pinning effect of the solutes and the high migration ability of these long boundaries contribute to this irregularity.

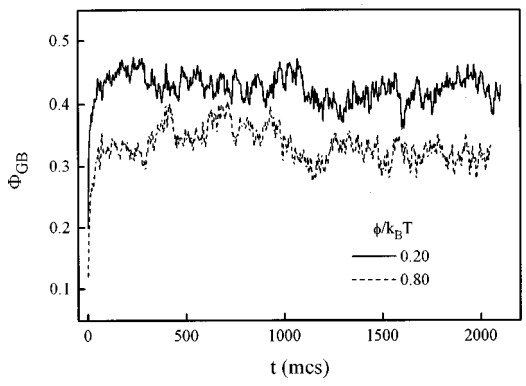

FIG. 6. The segregation coefficient Φ_{GB} as a function of time at two values of ϕ/k_BT for case II.

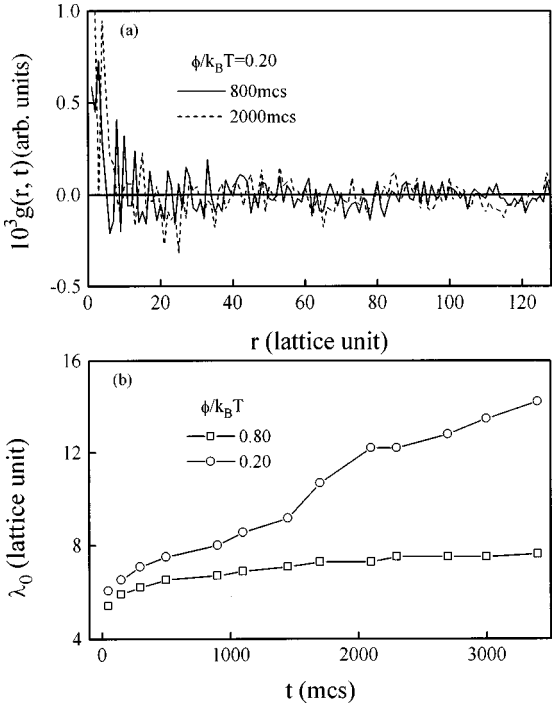

FIG. 7. (a) The radially averaged correlation function $g(r,t)$ as a function of r at $\phi/k_BT=0.20$ and (b) the fundamental wavelength λ_0 as a function of time at two values of ϕ/k_BT, for case II.

The evaluated segregation coefficient Φ_{GB} as a function of time is shown in Fig. 6. In reference to Fig. 3, case II has a lower Φ_{GB}. Looking at $g(r,t)$ as plotted in Fig. 7(a), one does not find an additional modulation scale besides the characteristic length λ_0, although λ_0 grows gradually with time, as shown in Fig. 7(b). Both λ_0 and its growth are lower in case II than in case I. All of these appear to provide evidence that the weaker segregation is achieved in the case of the higher ability of domain-boundary migration.

C. Scaling law of domain growth

The most distinguished property of the domain growth is the scaling law of the domain size distribution with respect to its average size $\langle A\rangle$.[3–5] We will check the scaling in the case of the domain-boundary segregation involved. The data are evaluated and presented in Fig. 8 for case I. As is clearly seen, the rescaled distribution curves $f(A/\langle A\rangle,t)$, at several

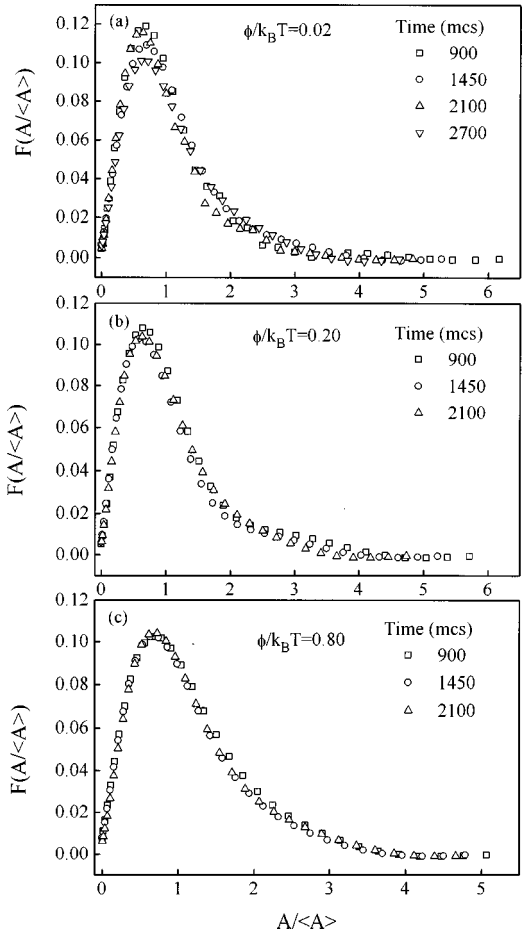

FIG. 8. The rescaled distribution functions of the domain area A at several times ($t \geqslant 900$ mcs) for case I. (a) $\phi/k_BT=0.02$, (b) $\phi/k_BT=0.20$, (c) $\phi/k_BT=0.80$.

times after $t=900$ mcs, fall onto the same curve $F(A/\langle A\rangle)$ within the statistical uncertainty. For case II, the same scaling is constructed. The scaling property of the domain growth, in the case of the existence of the domain-boundary segregation, is demonstrated in our simulation.

Nevertheless, a careful processing of the data shows that the scaling function $F(A/\langle A\rangle)$ depends on ϕ/k_BT. Evaluating the peak height F_M and the full width at half maximum (FWHM) as a function of ϕ/k_BT, one finds a slight decay of F_M and a slow growth of the FWHM, as plotted in Fig. 9. An

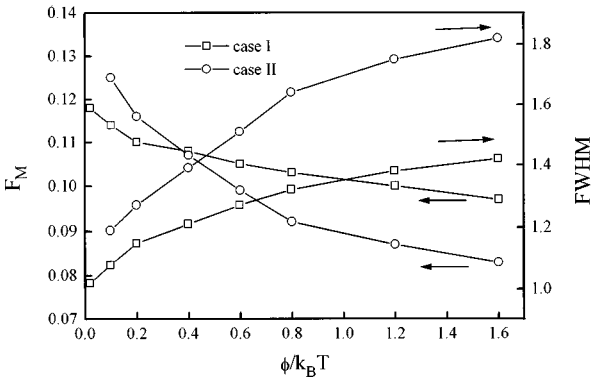

FIG. 9. The peak value F_M and the FWHM of the scaling function $F(A/\langle A\rangle)$ as a function of ϕ/k_BT for cases I and II.

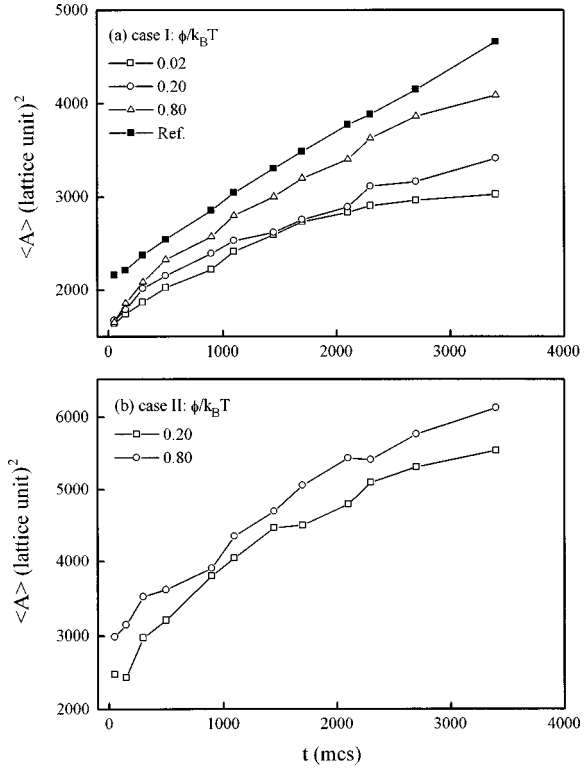

FIG. 10. The kinetics of domain growth at several values of ϕ/k_BT for (a) case I and (b) case II. In (a) the solid squared dots (—■—Ref.) are the data from the normal domain growth.

acceptable explanation of this fact is that the domain growth becomes easier as ϕ/k_BT is higher, so that the distribution exhibits a wide FWHM and a lower F_M, because the pinning effect of solutes is weaker at higher ϕ/k_BT. Irregardless of this, no big difference of the dependence tendency between cases I and II is detected, in spite of a higher FWHM and a lower F_M in case II due to the high ability of the boundary migration.

D. Kinetics of domain growth

It was mentioned earlier that because of the nonconserved Potts spin states, the domain growth can be characterized kinetically by a linear law of the growth of $\langle A\rangle$. We present the evaluated data of $\langle A\rangle$ as a function of time for all systems simulated. The results are plotted in Fig. 10. For a comparison, we insert in Fig. 10(a) the data achieved, in case of no domain boundary segregation ($f_{BB}=1.0$), as labeled with solid squared dots.

When the domain growth, in case of no boundary segregation, indeed shows a linear dependence of $\langle A\rangle$ on time, quite different behaviors are observed for both cases I and II. First, the time dependence of $\langle A\rangle$ shows a considerable negative deviation from the linear law. This deviation becomes greater at a lower value of ϕ/k_BT. Secondly, $\langle A\rangle$ decreases with decreasing ϕ/k_BT. By fitting the data for cases I and II with a power law,

$$\langle A\rangle \propto t^n, \tag{14}$$

where n is the growth exponent. It varies from 0.80–0.30 as ϕ/k_BT changes from 0.80 to 0.02. This result demonstrates

that the normal kinetic law for domain growth is no longer applicable in case of the domain-boundary segregation.

E. Remarks

We have simulated, in detail, the domain-boundary segregation of the solutes in parallel to the domain growth. By choosing the system parameters we are shown strong coupling between the segregation and domain growth. This is the first simulation on the coupling phenomenon although they have been revealed by a number of experimental investigations.

What we should point out here is that the MC algorithm developed above still has space to improve. We were supposed to choose the site at which either the Ising event or the Potts event will be initiated. In fact, we may develop another importance sampling for choosing a lattice site. This sampling considers the probability of an individual site for the next sequence. It can be written as

$$P=\frac{\exp[-(E_I+E_P)/k_BT]}{\exp(H/k_BT)}. \tag{15}$$

Therefore, the site of the smallest (E_I+E_P) has the highest probability to be chosen for either the Ising or Potts operation.

For the relaxation in a system of nonconserved spin states, such as the domain growth, the kinetics is much faster than that in a system of conserved spin states, such as diffusion. Therefore, the spin state conservation limits the relaxation in component diffusion, whereas domain evolution in a highly degenerated system proceeds in a more developed manner so that a higher kinetic exponent is achieved. In our simulation, we consider a coupling between a conserved system and a nonconserved one. It is found that the latter can be modulated in kinetics, resulting in an exponent smaller than the normal exponent in a homogeneous lattice.

When we deal with a system of $\phi/k_BT<0$, the situation becomes more complicated. We must treat both phase precipitation and domain growth as parallel and coupling processes. An extension of our model is direct in this case. It is expected that both the kinetic law of domain growth[6–9] and the Lifshitz-Slyozov-Wagner law[22,23] of phase separation have to be modified. This relaxation process will be of special interest and is the object of further study.

IV. CONCLUSION

In summary, we have developed a MC approach of domain-boundary segregation in polycrystalline solid solutions. Our approach starts from the kinetic Ising model and Q-state Potts model and propose an algorithm of simulating the coupling between solute diffusion and domain growth so that the domain-boundary segregation can be developed. The serious segregation of the solutes onto the DBs in a two-dimensional squared binary lattice has been demonstrated when the Potts interaction between solute pairs is modulated. The segregation behaviors have been characterized by various evaluations. It has been revealed that the segregation on the DBs depends on the effective Ising interaction and migration ability of the DBs. We have demonstrated the scaling property of domain growth in the case of the domain-boundary segregation. The domain growth exhibits negative deviation from the normal growth kinetics as in a homogeneous binary system without domain-boundary segregation.

ACKNOWLEDGMENT

The author would like to thank the National Natural Science Foundation of China for partial support of this work.

*Present address: Institute of Materials Research and Engineering, Blk. S7, Level 3, Science Drive 4, National University of Singapore, Singapore 119260. Electronic address: liujm@imre.org.sg

[1] P. Haasen, *Physikalische Metallkunde* (Springer-Verlag, Berlin, 1984).
[2] G. S. Grest, M. P. Anderson, and D. J. Srolovitz, in *Computer Simulation of Microstructural Evolution*, edited by D. J. Srolovitz (AIME, Warrendale, Pennsylvania, 1986), p. 21.
[3] J. Stavans, Rep. Prog. Phys. **56**, 733 (1993).
[4] V. E. Fradkov and D. Udler, Adv. Phys. **43**, 739 (1994).
[5] W. W. Mullins, J. Appl. Phys. **59**, 1341 (1986).
[6] P. S. Sahni, D. J. Srolovitz, G. S. Grest, M. P. Anderson, and S. A. Sahni, Phys. Rev. B **38**, 2705 (1983).
[7] M. P. Anderson, D. J. Srolovitz, G. S. Grest, and P. S. Sahni, Acta Metall. **32**, 783 (1984).
[8] M. P. Anderson, G. S. Grest, and D. J. Srolovitz, Scr. Metall. **19**, 225 (1985).
[9] G. S. Grest, M. P. Anderson, and D. J. Srolovitz, Phys. Rev. B **38**, 4752 (1983).
[10] P. Gordon and T. A. El-Bassiouni, Trans. Soc. Min. Eng. AIME **233**, 399 (1965).
[11] W. W. Mullins, Acta Metall. **6**, 414 (1958).
[12] G. F. Bolling and W. C. Winegard, Acta Metall. **6**, 288 (1958).
[13] G. Gottstein and L. S. Shvindlerman, Scr. Metall. **27**, 1515 (1992).
[14] G. R. Purdy, in *Materials Science and Technology: A Comprehensive Treatment*, edited by P. Haasen (VCH, New York, 1991), Vol. 5, p. 305.
[15] K. Kawasaki, in *Phase Transitions and Critical Phenomena*, Vol. 2, edited by C. Domb and M. S. Green (Academic, New York, 1972), p. 443.
[16] N. Metropolis, A. W. Rosenbluth, A. H. Teller, and E. Teller, J. Chem. Phys. **21**, 1987 (1953).
[17] F. Y. Wu, Rev. Mod. Phys. **54**, 235 (1982).
[18] K. Yaldram and K. Binder, Acta Metall. Mater. **39**, 707 (1991).
[19] K. Yaldram and K. Binder, J. Stat. Phys. **62**, 161 (1991).
[20] R. F. Xiao, J. I. D. Alexander, and F. Rosenberger, Phys. Rev. A **43**, 2977 (1991).
[21] R. F. Xiao, J. I. D. Alexander, and F. Rosenberger, Phys. Rev. A **45**, 571 (1992).
[22] I. M. Lifshitz and V. V. Slyozov, J. Phys. Chem. Solids **19**, 35 (1961).
[23] C. Wagner, Z. Elektrochem. **65**, 243 (1961).